Available online at www.sciencedirect.com

ScienceDirect

Energy Procedia 54 (2014) 185 – 198

Energy Procedia

4th International Conference on Advances in Energy Research 2013, ICAER 2013

Design Of A 16-Cell Densely-Packed Receiver for High Concentrating Photovoltaic Applications

Leonardo Micheli[a], Nabin Sarmah[a], Xichun Luo[b], K. S. Reddy[c], Tapas K. Mallick[a]*

[a]*Environment and Sustainability Institute, University of Exeter, Penryn Campus, Penryn, Cornwall TR10 9FE, UK*
[b]*Department of Design, Manufacture and Engineering Management, Faculty of Engineering, University of Strathclyde, Glasgow, G1 1XQ, UK*
[c]*Heat Transfer and Thermal Power Laboratory, Department of Mechanical Engineering, Indian Institute of Technology Madras, Chennai 600 036, India*

Abstract

A novel densely packed receiver for concentrating photovoltaics has been designed to fit a 125× primary and a 4× secondary reflective optics. It can allocate 16 1cm^2-sized high concentrating solar cells and is expected to work at about 300 W_p, with a short-circuit current of 6.6 A and an open circuit voltage of 50.72 V. In the light of a preliminary thermal simulation, an aluminum-based insulated metal substrate has been use as baseplate. The original outline of the conductive copper layer has been developed to minimize the Joule losses, by reducing the number of interconnections between the cells in series. Slightly oversized Schottky diodes have been applied for bypassing purposes and the whole design fits the IPC-2221 requirements. A full-scale thermal simulation has been implemented to prove the reliability of an insulated metal substrate in CPV application, even if compared to the widely-used direct bonded copper board. The Joule heating phenomenon has been analytically calculated first, to understand the effect on the electrical power output, and then simulate, to predict the consequences on the thermal management of the board. The outcomes of the present research will be used to optimize the design of a novel actively cooled 144-cell receiver for high concentrating photovoltaic applications.

Selection and peer-review under responsibility of Organizing Committee of ICAER 2013

Keywords: Solar energy, CPV, receiver, IMS, high concentration.

* Corresponding author. Tel.: +44-01326259465.
E-mail address: t.k.mallick@exeter.ac.uk

Selection and peer-review under responsibility of Organizing Committee of ICAER 2013
doi:10.1016/j.egypro.2014.07.262

1. Introduction

Photovoltaics represents the third most important renewable energy source in terms of globally installed capacity [1]. At the end of 2012, the global installed PV capacity reached 99 GW [2]. Since 1980, the photovoltaic market has grown by 37% per year [2] and, in 2011 and 2012, PV was the first electricity source for sizing of the new installations in Europe [1]. Even in front of such a remarkable development, the cost of the technology still represents a limit for the growth of the market [3,4]. The idea behind the Concentrating Photovoltaic (CPV) is to use refractive or reflective materials to focus the same irradiance on a smaller expensive semiconductor surface. In order to improve the efficiency of the system, multijunction cells are generally applied: these cells are made of more than one semiconductive layer. GaInP/GaAs/Ge cells represent the most common devices and have shown a record efficiency of 37.9% [6].

The increase in irradiance and reduction in volume lead to a rise in heat production. Considering an optical efficiency of 20% and a cell efficiency of 30%, a 500× system operating under Concentrating Standard Operating Conditions (DNI of 900 W/m2, [7]) is expected to produce about 25 W/cm2 of waste heat. Thermal management is a key issue for Concentrating Photovoltaic (CPV), since a drop in efficiency of about 0,035% per rise in Celsius degree is reported [5]. CPV plants exhibit even long-term degradation when working at high temperatures: they can safely work at any temperature below 80-100°C. Cooling is generally not required for concentration ratio below 5×, while is necessary in the other cases. Either active or passive cooling systems have be applied in different CPV systems [6,7].

In a CPV system, the receiver represent the element where the cells and the other surface mount components are place and in charge of heat and electrical power removal [8]. The choice of materials and components of the receiver plays a fundamental role both in the thermal management and in the cost of the product [9]. The receiver represents 20% of the cost of the whole CPV system, which includes the cooling system [10]. Printed Circuit Boards (PCB) are the most common board in electronic applications, due to their high flexibility and relatively low costs. PCBs are laminated material bonded with heat cured flame retardant epoxy resin and clad on either one or both sides with copper. Usually the laminated material is a low thermal conductive fiberglass, but it can be replaced with a metal baseplate: this case the thermal management of the system can be enhanced and the board is called Insulated Metal Substrate (IMS). The metal base works for mechanical support and for heat spreading: an electrical insulating film is placed between the base and the conductive layer. Aluminum is the material generally chosen as baseplate, due to its excellent thermal conductivity, light weight and relatively low cost [11]. IMSs have been developed to be used in LED (Light Emitting Diode) applications and show an heat transfer management similar to the one needed by the CPV technologies [12]. The CPV receiver manufacturers' interest on this technology is increasing [12–15]. In this light, Mabille et al. [13] demonstrated that, when exposed to accelerated aging tests, IM substrates behave as the Direct Bonded Copper (DBC) boards, the most used substrates in CPV applications [16–19]. The exploitation of IMS can positively affect both the thermal management and the cost of the CPV devices.

In this paper the design of a new 16-cell receiver for 500× CPV applications is presented. The copper pattern has been conceived to minimize the electrical resistivity and to make the prototype easily scalable. An aluminum based insulated metal substrate is considered as baseplate: a preliminary thermal simulation has been run before starting the work, to compare the performances of an IMS and a more expensive DBC. A full scale simulation, inclusive of the heat production due to the Ohm losses, has then been run to demonstrate the reliability of IMS in a densely packed high CPV system. The presented design can represent a step toward the required reduction in price of CPV systems and will be used to conceive a new 144-cell receiver.

Nomenclature

A	Conductor's cross section surface (m^2)
C_p	Heat capacity (J/kgK)
E	Electric field strenght (kg m/s^3A)
I	Electric current (A)
J	Current density (A/m^2)
l	Length of the conductor (m)

k	Thermal conductivity (W/mK)
N_{cell}	Number of cells on the plate
P_{el}	Electric power output (W_e)
P_{cell}	Waste heat produced by one cell (J)
Q	Heat generated due to limited cell efficiency and Joule losses (J)
Q_J	Heat generated due to Joule losses (J)
R	Electrical resistivity (Ω)
T_{ext}	External temperature (K)
T_s	Surface's temperature (K)
V_{scm}	Total semiconductive material on the plate (m^3)
ρ	Density (kg/m^3)
ρ_{el}	Electrical resistivity (Ω m)
σ	Electrical conductivity (S/m)

2. CPV system configuration and receiver

2.1. System description

In present work a 10×10 cm IMS board has been developed to allocate 16 cells. The receiver is being developed as part of a 10 kW_e high concentrating photovoltaic system, developed by the University of Exeter and the Indian Institute of Technology Madras. The CPV is conceived the work at a concentration of 500 suns. The geometry of the system is composed by two reflective optics (Fig. 1). A 3×3m primary mirror focuses the irradiance by 125 times onto the 26.8×26.8cm surface of the secondary optics. The secondary uniformly spreads the sunlight across the cells, increasing the concentration four more times. A tracking system will be installed to keep the optics and the receiver in the best position and to optimize the energy cell's production. The receiver is coupled to a water-based active cooling system [20], which is placed on the back of the plate.

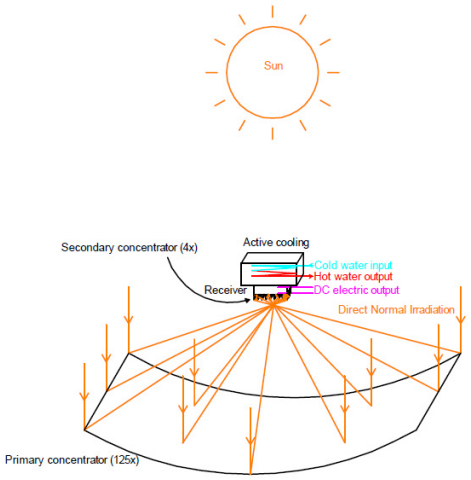

Fig. 1. Schematic of the CPV system

2.2. Surface-mount components

Azurspace's 3C40 cells [5] were considered for this application. These GaInP/GaAs/Ge cells are grant efficiencies up to 37.2% at 500×. At their 500× maximum power point, they generate 6.400 A at 2.889 V. The whole setup counts 16 series-connected cells and is expected to show a peak power of about 300 W_e, with a short-circuit current of 6.587 A and an open-circuit voltage of 50.72 V. Each cell sizes 11x10 mm, but the active area is limited to 10×10mm, because of two 0.45mm-width tabs on the front.

In order to maximize the performances of the system, one bypass diode per cell is going to be applied [21]. The Vishay V10P45S Schottky rectifier has been chosen due to the good compromise between dimensions and performances. Schottky diodes are usually employed as bypass devices for multijunction cells: they have a lower forward voltage drop and, therefore, lower losses and lower temperature while in bypass operation than the one of the silicon ones. The diodes have been slightly oversized to obtain a low increasing in reverse voltage and to reduce the risks of breaking: diodes can easily break if working closer to the maximum rating. Taking into account the cell's short circuit current (6.587 A), a 10 A Schottky diode grants an acceptable safety factor of 1.52. The diodes applied in the systems are surface-mount diodes (SMD), because cheaper and easier to replace than the discrete ones [22]. The V10P45S diode requires a mounting pad surface of 6.80×4.80mm and is about 1.1mm high.

2.3. The materials

The IMS has a 1.6 mm thick aluminum baseplate and a 35 µm-thick copper layer, bonded together with a 4.5 µm thick marble resin. All the surface mounted components will be soldered using a Sn96,5/Ag3,5 solder paste. The board has been developed using a chemical etching process and is shown in Fig. 2. Two main processes can be used to produce the printed circuit boards: chemical etching or mechanical milling. This case the first one has been used: it grants higher precision even if it has a lower repeatability than the mechanical one. The chemical process is made of different steps. Firstly, the laminate is exposed period under a high resolution UV lamp, using a mask. Immediately after the exposure, the laminate is immersed into a developer, where the photosensitive resin previously exposed is removed by the developer solution. The board is then moved into an etching tank, in which a pre-heated etchant solution removes the copper which is no longer protected by the resin. At the end, the laminate is re-exposed under the UV lamp and then immersed into the developer solution: the resin is then removed and the circuit is complete.

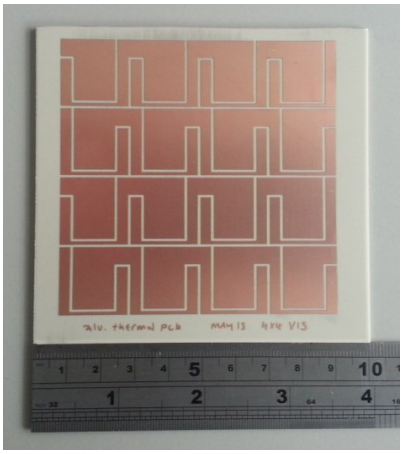

Fig. 2. The design printed onto a 10×10cm IMS board

3. Electrical analysis of CPV receiver

The original design of the copper pattern has no intermediate interconnections between the negative pad of a cell

and the negative one of the following cell: as shown in Fig. 3, one shape of copper is used for both purposes. This allows lowering the electrical resistivity of the copper and, then, the electrical losses. The design has been drawn up accordingly to the IPC-2221 Generic Standards on Printed Board Design [23]. A copper width of at least 3.0 mm has been considered where a current of 6.6 A is supposed to flow, while at least 0.7 mm have been considered where only half of the current is flowing (Fig. 3).

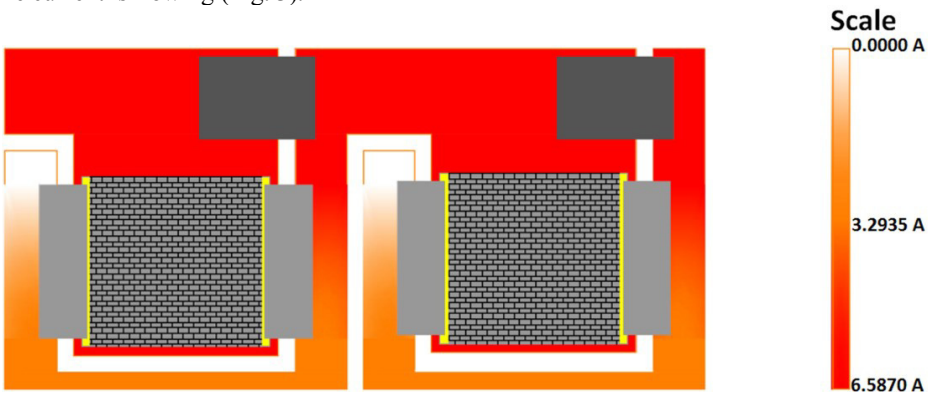

Fig. 3. Current distribution across the receiver design

Using the results shown in Fig. 3, it is possible to estimate the electric losses due to the Ohm's law. The whole receiver is made of three different copper shapes repeated in space: they are shown in Fig. 4 and have been named C1, C2 and C3. The copper pattern is divided in 20 components: C1 and C3 are placed at the beginning and at the end of each row, while a series of three C2 forms the remainder part of it.

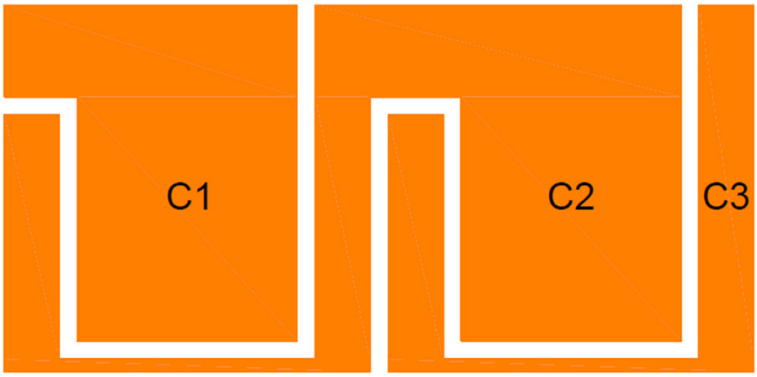

Fig. 4. The three copper shapes: C1, C2, C3.

The conductive layer has a thickness of 35 μm and an electrical resistivity (R) of 1.62×10^{-8} Ω·m can be expected. The analytical investigation was carried out based on the definition of Ohm's law [24], and is given as:

$$V = I * R \tag{1}$$

The resistance (R) is expressed as follow [24]:

$$R = \rho_{el} * \frac{l}{A} \tag{2}$$

In any direct current system, the power (P_{el}) can be obtained as:

$$P_{el} = V * I = R * I^2 \quad (3)$$

The equation in (3) has been used to calculate the power lost due to Ohm's law. The losses has been calculated separately for each copper shape and then summed: all the values are reported in Table 1. About 4.22 W are expected to be lost, out of an overall electrical capacity of about 335 W_e. This means that 1.2% of the electrical output is lost converted into waste heat in the copper layer.

Table 1. Ohmic losses per conductive component.

Component	Power lost per piece [W]	No of pieces per board	Power lost per component [W]
C1	0.0264	4	0.1055
C2	0.2564	12	3.077
C3	0.2596	4	1.038

According to the Standards [23], the presented 35 μm-thick copper layer is fine when working at temperatures at least 40°C higher than the ambient temperature. Considering an ambient temperature of 25°C, the system is allowed to work at 65°C or over, which is the range in which the concentrating photovoltaic cells usually operate [25]. On the other hand, using a 70 μm-thick copper layer, the system is able to work with any temperature higher than 35°C. All these dimensions have been calculated taking into account both adequate 10%-tolerances and the effect of the thermal expansion at the maximum allowed cell's operating temperature (150°C). A gap of 1 mm is considered between the negative and the positive pad of each cell and between each row: this distance is above the minimum value recommended by the standards (0.13 mm).

4. Thermal analysis of CPV receiver

4.1. Simulation setup

Each cell produces about 20-25W of waste heat when operates at 500×. So far, the commercial assemblies have been based on DBC, which grant excellent thermal and mechanical properties. In the present study, three potential backplates has been considered: a PCB, a DBC substrate and an IMS. A preliminary three dimensional simulation has been run in COMSOL Multiphysics 4.3a to compare their thermal behaviors. The single-cell receiver has been built in the software: the solar cell (CC) was placed onto the copper layer (CL), which is accommodated onto the 20×20 mm heat sink through a dielectric layer. Interconnectors (IC) were modeled as 0.025 mm-thick silver tabs. The diode (D) was not considered for this thermal simulation, due to the negligible current flowing into it when the system is in operation.

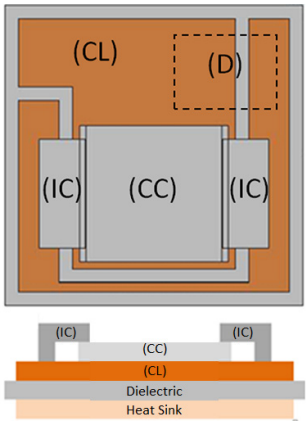

Fig. 5. Front view and cross section of the single cell receiver developed in COMSOL.

The thicknesses of the layers have been established on the basis of commercially available products and are reported in Table 2.

Table 2. Thicknesses of the different layers in the three developed receiver

Layer	Printed Board Circuit	Direct Bonded Copper	Insulated Metal Substrate
Interconnectors	0.025mm-thick silver	0.025mm-thick silver	0.025mm-thick silver
Cell	0.190mm-thick germanium	0.190mm-thick germanium	0.190mm-thick germanium
Conductive layer	0.035mm-thick copper	0.30mm-thick copper	0.035mm-thick copper
Dielectric	4.5um-thick marble resin	0.63mm-thick AlN	4.5um-thick marble resin
Heat sink	1.6mm FR-4 fiberglass	0.30 mm-thick copper	1.6mm-thick aluminum

4.2. Materials' properties

A pure thermal simulation requires in input the values of the thermal conductivity, the density and the heat capacity at constant pressure per each material. A Joule heating simulation was run only for the insulated metal substrate: in this case, the electrical conductivity and the relative permittivity are needed as well. Wherever possible, the COMSOL built-in materials were chosen: this is the case of aluminum and copper. The other materials and the relative properties have been added from the user: the introduced values are reported in Table 3. The marble resin, which acts as a dielectric in the PCB and the IMS, has been modeled as a thin thermally resistive layer: a thickness of 0.0045 mm and a thermal conductivity of 3 W/mK have been considered. The cell has been assumed to be completely made of germanium, in accordance with the previous literature [26,27].

Table 3. Materials' properties (Materials marked with * are COMSOL built-in materials)

Material	Thermal Conductivity, k [W/mK]	Density, ρ [kg/m^3]	Heat Capacity, C_p [J/kgK]	Electrical Conductivity, σ [S/m]	Relative Permittivity
Aluminum Nitride	285	3260	740	-	-
Aluminum*	160	2700	900	$5.998*10^7$	1
Copper*	400	8700	385	$3.774*10^7$	1
FR-4	1.7	1850	600	-	-
Germanium	60	5323	320	2000	1
Silver	430	10490	235	-	-

4.3. Governing equations and boundary conditions

The simulation was developed using the COMSOL's "Heat Transfer in Solids" module. The cell has been set as heat source to model the conversion of part of the sunlight into waste heat Considering a DNI of 850W/m^2, a cell efficiency of 40% and an optical efficiency of 90%, an overall heat production of 22.95 W per cell (P_{cell}) was predicted at 500×. The heat exchange is based on conduction between the solid layers (4) and the expression derives from the Fourier's law [28]:

$$\nabla\left(-k\nabla T\right)=Q \tag{4}$$

where ∇ is three dimensional del operator. This element has been calculated from P_{cell} taking into consideration the number of cells on the plate (N_{cell}) and their total volume (V_{scm}):

$$Q=\frac{P_{cell}*N_{cell}}{V_{scm}} \tag{5}$$

At the bottom of the plate, a uniform convective cooling has been considered, to stand for the active cooling used in the real case scenario. An heat transfer coefficient of 10^4 W/m^{2}K was considered: this is the minimum value to be considered for over 150 suns densely-packed systems according to Royne et al. [6]. The equation (6), based on the Newton's law of cooling [28], explains how this condition is modeled, taking into account the difference between the external and the board surfaces (T_{ext} and T_s respectively).

$$-\overline{n}*\left(-k\nabla T\right)=h*(T_{ext}-T_s) \tag{6}$$

Excepted for the surface on the backside of the plate, all the other media-facing surfaces were model as adiabatic surfaces:

$$-\overline{n}*\left(-k\nabla T\right)=0 \tag{7}$$

Where the effects of the Ohm losses are modeled, the "Joule Heating" module was exploited. This feature is based on a modified version of the heat equation at the steady state (4). In this case, the definition of Q changes and the electromagnetic losses (Q_J) are added as boundary heat sources in the heat transfer computation:

$$Q=\frac{P_{cell}*N_{cell}}{V_{scm}}+Q_J \tag{8}$$

Q_J is the heat generated by the electric current. The expression derives from the Ohm's law [24] and is reported below:

$$Q_J=\overline{J}\cdot\overline{E} \tag{9}$$

where J is the current density and E is the electric field strength. It is equal to the potential gradient between the charged object and the ground, and opposite in direction [24]:

$$\overline{E} = -\nabla V \tag{10}$$

A current (I) of 6.587 A is imposed through the cells and the copper pattern. The magnitude of current density in a conductor with cross-section area A is given by [24]:

$$J = \frac{I}{A} \tag{11}$$

All the surfaces facing the air and the dielectric have been considered electrically insulated (12).

$$-n \cdot \overline{J} = 0 \tag{12}$$

4.4. Preliminary thermal simulations

The simulation was processed to predict the steady-state and has been developed to estimate the temperatures across the surfaces of the PCB, the DBC and the IMS. All the boards were tested in the same conditions. The overview of the outcomes are shown in the following pictures: each figure exhibits the temperature ditribution on the left side and the isothermal contours on the right one, both of them expressed in Kelvin. The PCB (Fig. 6) shows a peak temperature of 419.75 K. The DBC (Fig. 7) shows a maximum temperature of 303.1 A. The IMS (Fig. 8) reaches temperatures up to 305.13 K.

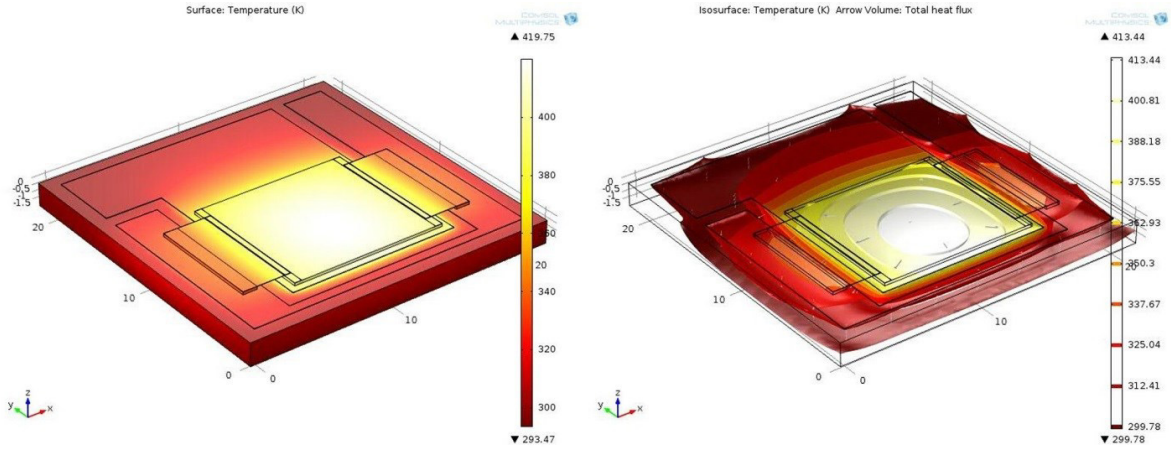

Fig. 6. Temperature distribution in the PCB based receiver.

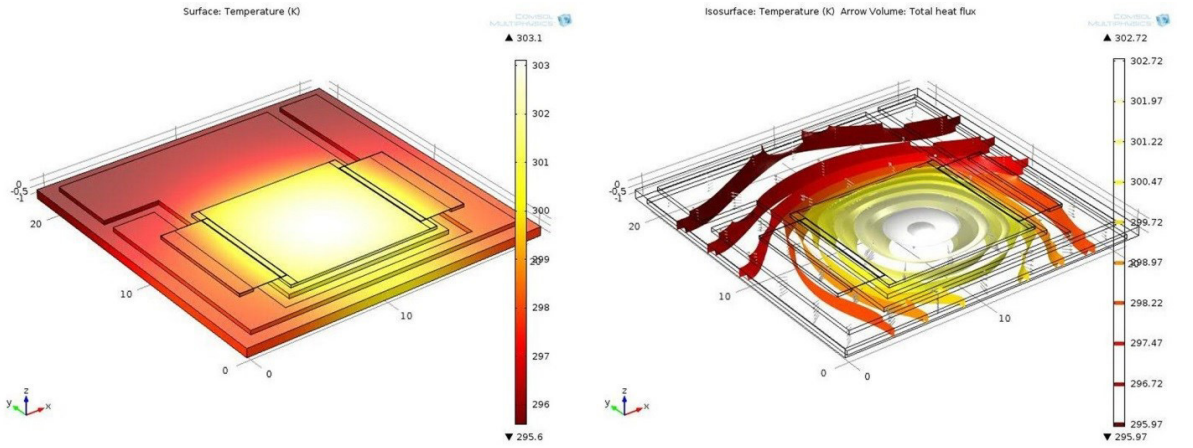

Fig. 7. Temperature distribution in the DBC based receiver.

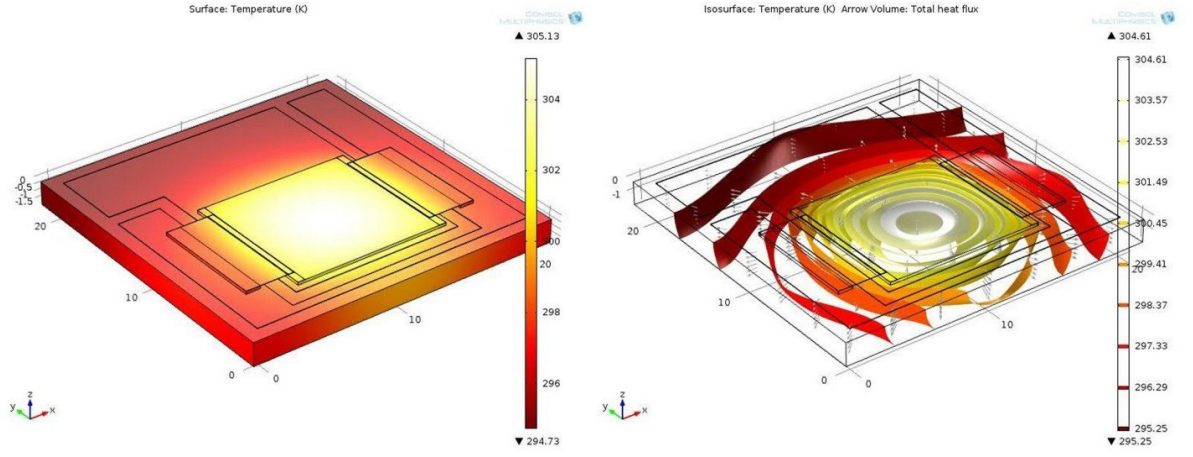

Fig. 8. Temperature distribution in the IMS based receiver.

As expected, the PCB based receiver is the worst performing. In the studied setup, it reaches a maximum temperature of 146.6 C, more than 100 degrees higher than the ones reported by the DBC and IMS receivers, and few tens higher than the conventional CPV operating temperature [25]. The isothermal contours are quite horizontal, due to the high thermal insulation provided by the fiberglass. Thus, PCB cannot be considered as a reliable backplate for high CPV applications, even in presence of a high performance active cooling. On the other hand, the thermal behaviors of the DBC and of the IMS receivers are comparable and definitely acceptable: in both the situations, the temperature doesn't exceed 40°C. For the purposes of this preliminary research, the simulation proves that an aluminum based IMS can be used to replace a higher-priced DBC in the current 500× CPV receiver.

4.5. 16-cell board thermal simulations

A full scale simulation has been run to attest the consistency of the whole receiver. The 16-cell receiver has been built in a COMSOL Multiphysics 4.3a environment, assuming the same hypotheses accounted in the previous simulations. Both the IMS and the DBC boards have been tested, in order to get a full scale comparison between them. The pictures below illustrate the outcomes of the simulations. In particular, Fig. 9 and Fig. 10 display the

temperatures on the surfaces of the boards and the cells. Any figure exhibits a top view on the left hand side and a 3D view on the order side. The results of the IMS are always reported first, followed by the DBC ones.

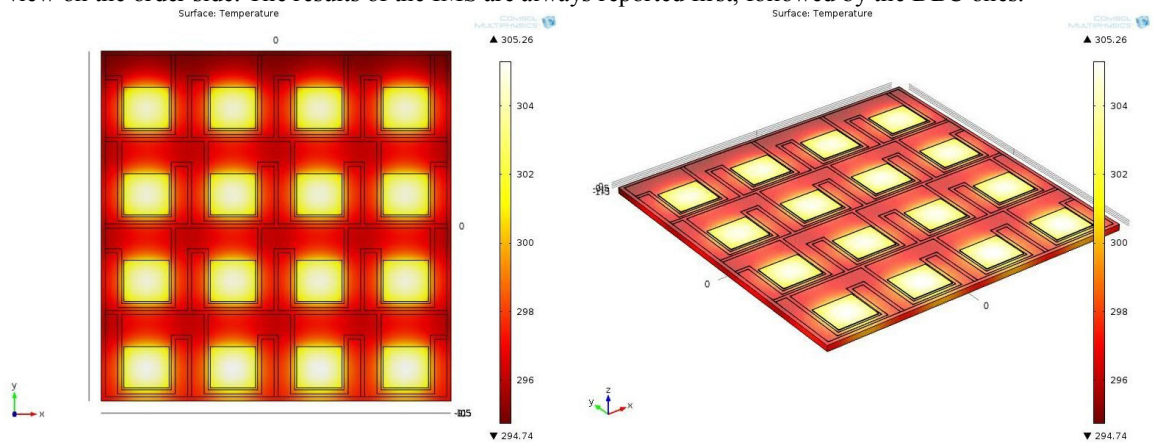

Fig. 9. IMS densely packed receiver's thermal simulation

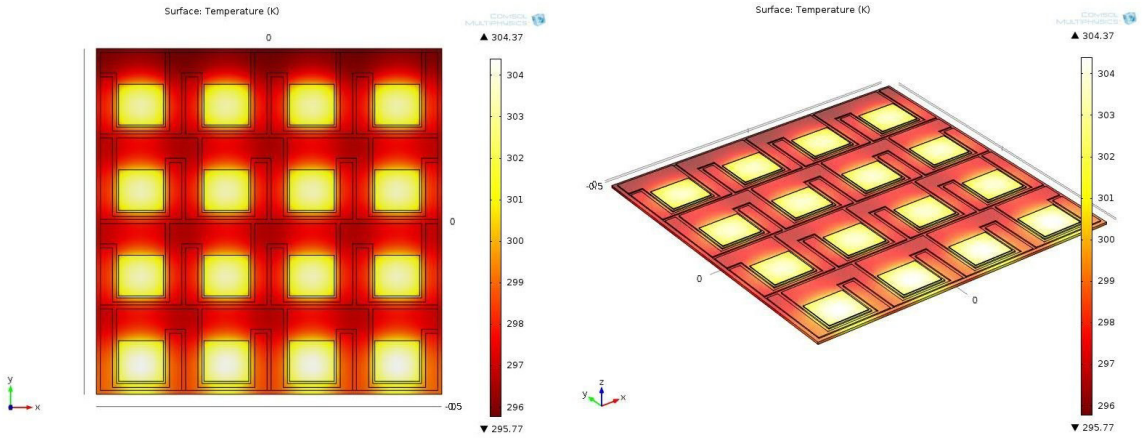

Fig. 10. DBC densely packed receiver's thermal simulation

Both the IMS and the DBC show maximum temperatures similar to the single cell case: the IMS reaches 305.26 K, while the DBC rises up to 304.37 K. As expected, the DBC is still performing better the IMS, but the difference in temperature can however be considered negligible. These results prove that an aluminium based insulated metal substrate can handle the waste heat produced by 16 multijunction cells at 500x disposed in a densely packed configuration. For a wider overview, the temperature contours of the IMS and the DBC board are shown in Fig. 11 and Fig. 12 respectively.

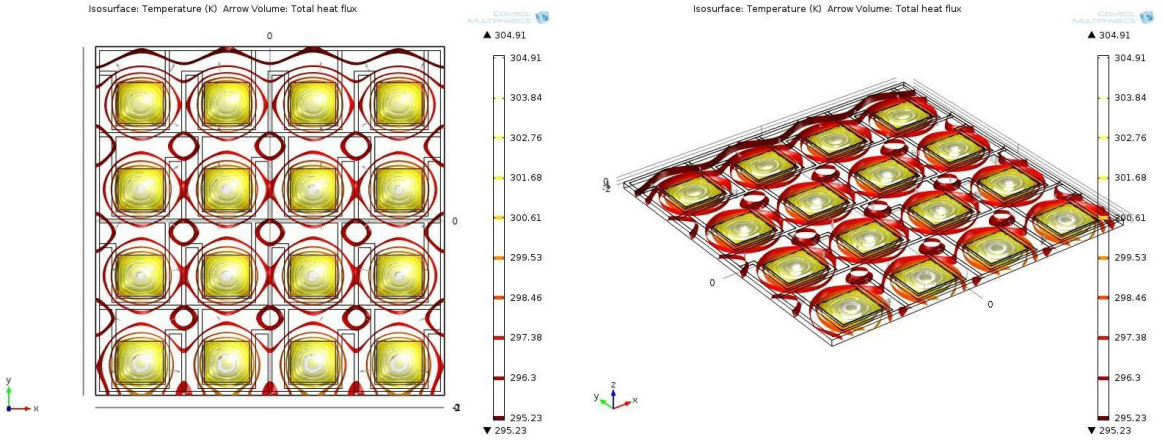

Fig. 11. Isothermal contours in the IMS receiver

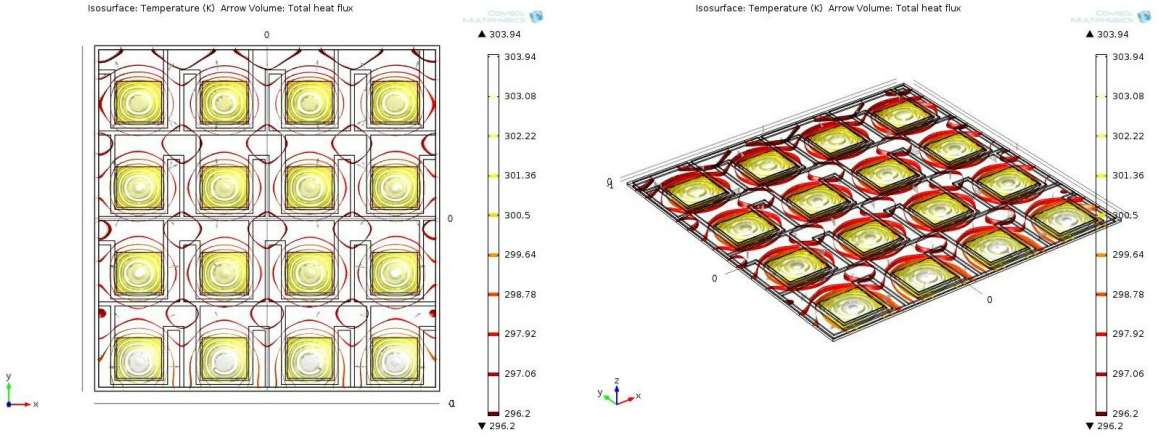

Fig. 12. Isothermal contours in the DBC receiver

In order to enhance the comprehensiveness of the investigation, the results of a simulation on the effect of the Joule heating on the IMS performances is reported as well. In this case, a current of 6.587 A has been set to flow in all the conductors and the cells. A negligible temperature rise has been recorded compared to the previous case and it is shown in Fig. 13, confirming once more the potential ability of an insulated metal substrate to manage the thermal management of a 500× CPV installation.

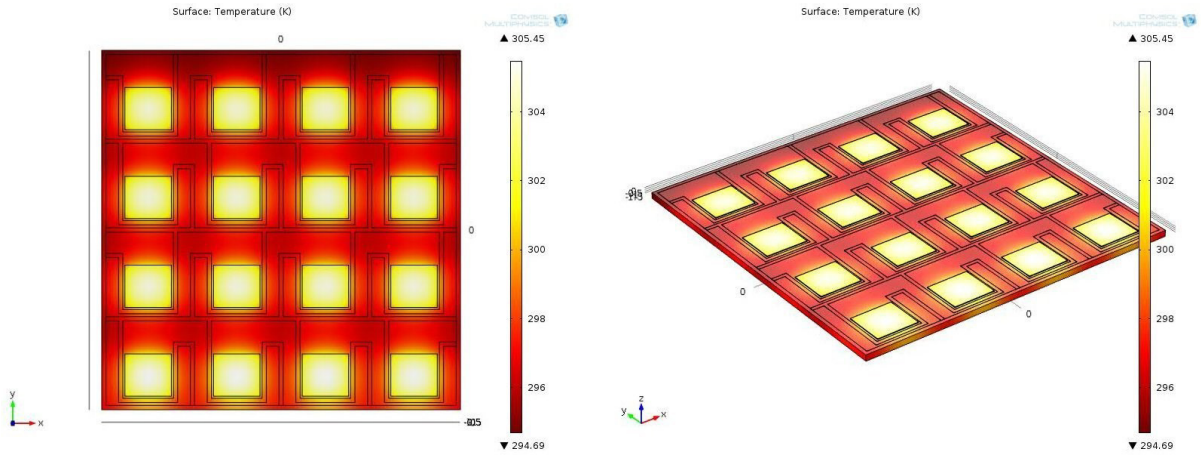

Fig. 13. IMS densely packed receiver's thermal simulation considering the Joule heating

5. Conclusions

An original 300 W_p receiver for 500× CPV application is presented in this paper. It has been conceived to work with a 125× primary and a 4× secondary optics and can allocate 16 one-square-centimeter cells. This assembly represents an innovation in the field for the novel low-resistance conductive pattern. The pattern is made of three copper shapes repeated in space: it can be easily scaled to accommodate a different number of cells. A preliminary three-dimensional simulation demonstrated the reliability of the IMS based assembly: the simulation's outcomes show that IMS behaves similarly to a DBC board in terms of heat removal. All the components have been designed to meet the Standards restrictions: the gap between the conductors grant enough insulation and the thickness of the copper can safely carry the expected current output. The shape of the electrically conductive layer has been conceived to reduce the resistance and then improve the electrical performances: it has been obtained decreasing the number of interconnections. The use of Slightly oversized Schottky diodes have been considered because of the good performances and the affordable safety factor they grant. The electrical and thermal behaviors have been proved using a full scale simulation: the receiver shows good thermal performances when cooled with an active cooling system, even if compared to a DBC board. The exploitation of an IMS will give an experimental contribution in the discussion about their reliability in CPV applications. The presented outline will be used to optimize the design a new actively cooled 144-cell receiver and to test the employability of aluminum micro-fins array as passive cooling system for CPV.

Acknowledgements

The financial support provided by the EPSRC-DST through the BioCPV project is duly acknowledged.

References

[1] Masson G, Latour M, Rekinger M. Global market outlook for photovoltaics 2013-2017. 2013.
[2] Werner C, Breyer C, Gerlach A. Analysis and Forecast of Global Installed Photovoltaic Capacity and Identification of Hidden Growth Markets. 28th Eur Photovolt Sol Energy Conf Exhib 2013:4733–49.
[3] Kurtz S. Opportunities and challenges for development of a mature concentrating photovoltaic power industry. 2009.
[4] Lund PD. How fast can businesses in the new energy sector grow? An analysis of critical factors. Renew Energy 2014;66:33–40.
[5] AZURSPACE Solar Power GmbH. 3C40 Concentrator Triple Junction Solar Cell datasheet 2010.
[6] Royne A, Dey C, Mills D. Cooling of photovoltaic cells under concentrated illumination: a critical review. Sol Energy Mater Sol Cells 2005;86:451–83.
[7] Micheli L, Sarmah N, Luo X, Reddy KS, Mallick TK. Opportunities and challenges in micro- and nano-technologies for concentrating photovoltaic cooling: A review. Renew Sustain Energy Rev 2013;20:595–610.

[8] IEEE-SA Standards Board. IEEE Recommended Practice for Qualification of Concentrator Photovoltaic (PV) Receiver Sections. 2001.
[9] Gombert A, Gmbh SS, Str B. Low Cost Reliable Highly Concentrating Photovoltaics – a Reality 2011:1651–6.
[10] Extance A, Marquez C. The Concentrated Photovoltaics Industry Report 2010. CPV Today 2010.
[11] Cordero N. Thermal Management of Bright LEDs for Automotive Applications. 7th Int Conf Therm Mech Multiphysics Simul Exp Micro-Electronics Micro-Systems 2006:1–5.
[12] Spirit Circuits Limited. Requirements of PCB's in solar & LED applications. EIPC Winter Conf. 2013, 2013.
[13] Mabille L, Mangeant C, Baudrit M. Development of CPV solar receiver based on insulated metal substrate (IMS): Comparison with receiver based on the direct bonded copper substrate (DBC) - A reliability study. AIP Conf. Proc., vol. 289, 2012, p. 289–93.
[14] Antonini A. Photovoltaic Concentrators - Fundamentals, Applications , Market & Prospective. In: Manyala R, editor. Sol. Collect. Panels, Theory Appl., Sciyo; 2010, p. 31–54.
[15] Cozzini M. Solar Cell Cooling and Heat Recovery in a Concentrated Photovoltaic System. 2012 COMSOL Conf. Milan, 2012.
[16] AZURSPACE Solar Power GmbH. Enhanced Fresnel Assembly - EFA 2010.
[17] Spectrolab Inc. CCA 100 C3MJ 1A Concentrator Cell Assembly 2011;91342.
[18] Emcore Corporation. CTJ Receiver Assembly – 5.5 mm x 5.5 mm 2011.
[19] Foresi JS, Yang L, Blumenfeld P, Nagyvary J, Flynn G, Aiken D. EMCORE receivers for CPV system development. 2010 35th IEEE Photovolt Spec Conf 2010:000209–12.
[20] Reddy KS, Lokeswaran S, Agarwal P, Mallick T. Numerical Analysis of Micro Channel Heat Sink Cooling System for Solar Concentrating Photovoltaic Module. 4th Int. Conf. Adv. Energy Res., Mumbai: 2013.
[21] Vorster FJ, van Dyk EE. Current-voltage characteristics of high-concentration, photovoltaic arrays. Prog Photovoltaics Res Appl 2005;13:55–66.
[22] Malvino A. Electronic Principles. McGraw-Hill; 2007.
[23] The Institute for Interconnecting and Packaging Electronic Circuits. IPC-2221 Generic Standard on Printed Board Design 1998:123.
[24] Warne DF. Newnes Electrical Engineer's Handbook. Newnes; 2000.
[25] Kinsey GS, Edmondson KM. Spectral Response and Energy Output of Concentrator Multijunction Solar Cells. Sol Cells 2009:279–88.
[26] Chow S, Valdivia CE, Wheeldon JF, Ares R, Arenas OJ, Aimez V, et al. Thermal test and simulation of alumina receiver with high efficiency multi-junction solar cell for concentrator systems. In: Schriemer HP, Kleiman RN, editors. Proc. SPIE 7750, vol. 7750, 2010, p. 775035–775035–8.
[27] Cancro C, Ciniglio G, Graditi G, Mongibello L, Pontecorvo A. Design and optimization of a novel heat dissipation system developed for ecosole C-PV modules. 28th Eur. Photovolt. Sol. Energy Conf. Exhib., Paris: 2013, p. 664–7.
[28] Incropera FP, DeWitt DP, Bergman TL, Lavine AS. Fundamentals of Heat and Mass Transfer. Wiley; 2007.